Journal of Magnetic Resonance **156,** 155–159 (2002)
doi:10.1006/jmre.2002.2546

COMMUNICATIONS

Intraresidue HNCA and COHNCA Experiments for Protein Backbone Resonance Assignment

Bernhard Brutscher

Institut de Biologie Structurale, Jean-Pierre Ebel C.N.R.S.-C.E.A., 41, rue Jules Horowitz, 38027 Grenoble Cedex, France

Received February 1, 2002; revised April 4, 2002

Two novel experiments, *intra*-HNCA and *intra*-COHNCA, are presented for sequential backbone resonance assignment of ^{13}C, ^{15}N labeled proteins. The advantage with respect to conventional pulse schemes is the suppression of the sequential $^{15}N \rightarrow {}^{13}C^{\alpha}$ coherence transfer pathway, which can be separately obtained from a HNCOCA correlation experiment. This results in a two-fold reduction of the number of detected correlation peaks. Spectral simplification is especially important for efficient automated assignment protocols as required in the context of high-throughput protein studies by NMR. The performance of the new experiments is demonstrated on an 18-kDa protein fragment of the *E. coli* sulfite reductase and compared to conventional techniques in terms of sensitivity and resolution.

Key Words: **HNCA; multidimensional NMR; protein; sequential resonance assignment; TROSY.**

NMR studies of protein structure, dynamics, or intermolecular interactions require as a first step resonance assignment of the protein backbone. Sequential backbone assignment of uniformly ^{13}C, ^{15}N enriched proteins is routinely obtained by recording a set of triple-resonance experiments correlating the frequencies of three different nuclei in a three-dimensional spectrum (*1–3*). Following the most commonly used protocols, pairs of experiments are recorded, e.g., HNCA and HN(CO)CA to connect the amide H(i) and N(i) frequencies with, in this case, the intraresidue $C^{\alpha}(i)$ and sequential $C^{\alpha}(i-1)$ nuclei. As in the HNCA experiment cross peaks are detected for both the intraresidue and sequential coherence pathways due to the similar size of the $^{1}J_{NC\alpha}$ and $^{2}J_{NC\alpha}$ coupling constants; the additional HN(CO)CA experiment is necessary to unambiguously identify the sequential correlation peaks. For larger proteins the increasing number of correlation peaks makes experiments attractive where more than three nuclei are correlated in one spectrum. The frequencies of four nuclei can be detected either by recording a four-dimensional NMR experiment or more conveniently by using ZQ/DQ spectroscopy where two frequencies are labeled in the same frequency dimension. This technique has also become known as reduced dimensionality spectroscopy (*4–6*). For example, the pair of experiments COHNCA (*7*) and HNCOCA (*8*) unambiguously connects the peptide plane nuclei H, N, and C′ with the C^{α} of the two residues involved in the peptide bond as long as the frequency triplet H, N, C′ is not degenerate. It has been shown in the past that the ZQ/DQ versions of these experiments are very helpful for sequential backbone assignment of folded or partially unfolded proteins (*9–12*).

The presence of both intraresidue and sequential correlation peaks, which increases the probability of accidental peak overlap in the spectrum, remains a drawback of HNCA and COHNCA. A single HNCA correlation peak detected for a given amide at the position of the corresponding HN(CO)CA cross peak may also be a source of confusion. It can be explained either by similar resonance frequencies of the intraresidue and sequential C^{α} carbons or by a missing intraresidue cross peak due to extensive C^{α} line broadening. To resolve these problems an experiment is needed which selectively correlates the H, N, and C^{α} nuclei of the same residue. This simplifies the HNCA (or COHNCA) spectrum by deleting the redundant sequential correlation peaks, independently obtained from the HNCOCA spectrum. In this Communication new pulse sequences, *intra*-HNCA and *intra*-COHNCA, are presented which largely suppress coherence transfer via the $^{2}J_{NC\alpha}$ coupling. In the resulting spectra only intraresidue H, N, C^{α} correlations yield cross peaks of significant intensity, which greatly enhances the resolution of the spectra and thus simplifies (automated) spectral analysis.

The pulse sequence shown in Fig. 1A is derived from the COHNCA experiment of Szyperski *et al.* (*7*) modified to suppress, or at least largely eliminate, the sequential H(i)–N(i)–$C^{\alpha}(i-1)$ coherence transfer pathway. The major difference is the insertion of a new pulse sequence element in the "out" and "back" $^{15}N \rightarrow {}^{13}C$ transfer steps between time points (a) and (b) and between (c) and (d). For the relevant coherence transfer pathways the ^{15}N transverse coherence, which is first allowed to evolve under the influence of the $^{1}J_{NC'}$, $^{1}J_{NC\alpha}$, and $^{2}J_{NC\alpha}$ couplings during a delay T, is converted into double- and zero-quantum coherence $2N_xC'_y$ by the 90° pulse applied on the

1090-7807/02 $35.00

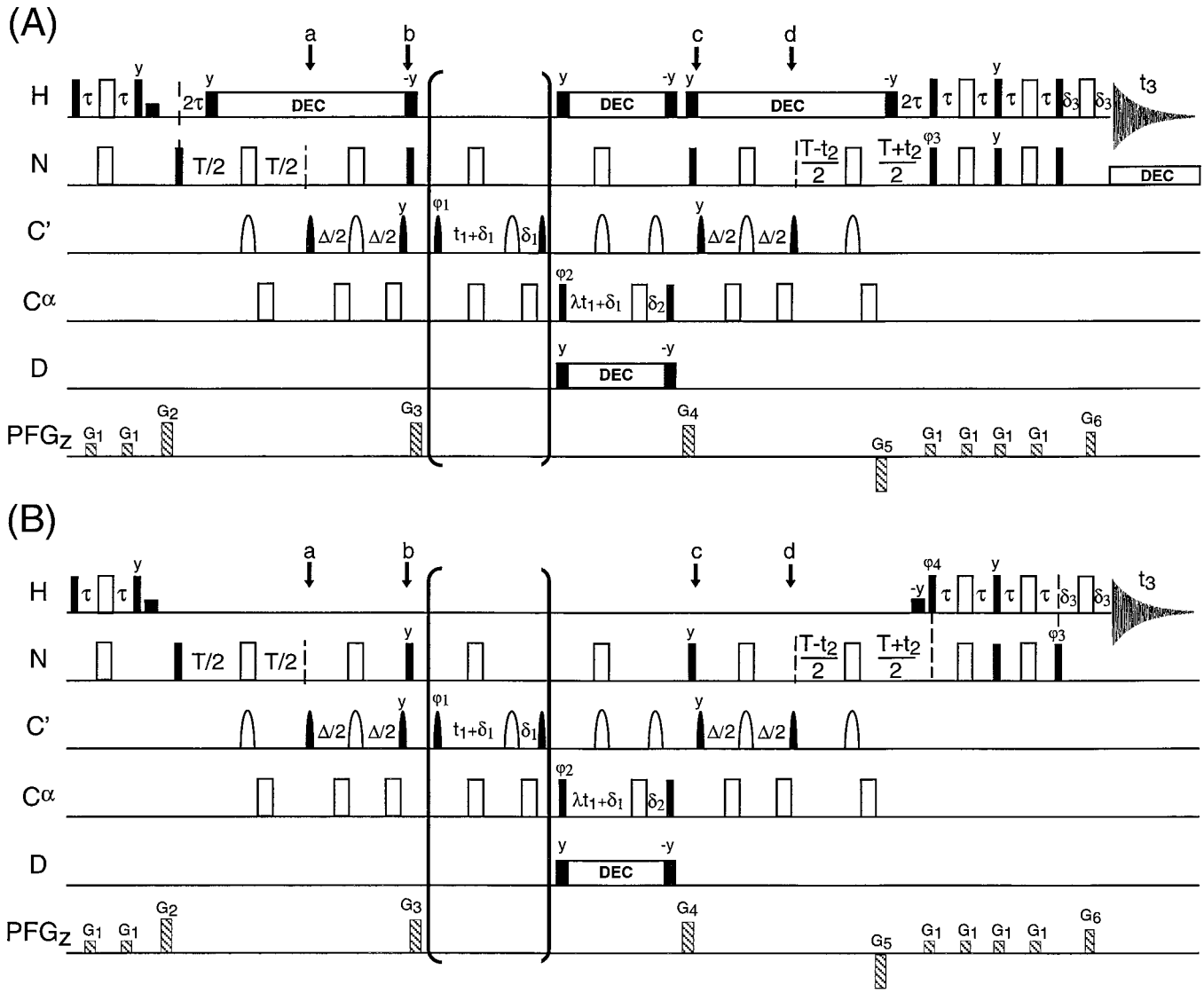

FIG. 1. Pulse sequences for (A) standard and (B) ^{15}N TROSY versions of the *intra*-HNCA and *intra*-COHNCA experiments. For the ZQ/DQ version of the *intra*-COHNCA experiment the C′ and C$^{\alpha}$ spins are frequency labeled in the same indirect frequency dimension (ω_1). For C$^{\alpha}$ frequency labeling the ^{13}C carrier is switched from the C′ to the C$^{\alpha}$ spectral region. The scaling factor λ determines the separation of the ZQ and DQ peaks (see Ref. *5*). If no additional C′ frequency labeling is desired (*intra*-HNCA) the pulses and delays inside the brackets are omitted. All radiofrequency (RF) pulses are applied along the x-axis unless indicated. The phases φ_1 and φ_2 are initially set to x, whereas $\varphi_3 = x$ for pulse sequence (A) and $\varphi_3 = -y$, $\varphi_4 = -x$ for pulse sequence (B). 90° and 180° RF pulses are represented by filled and open pulse symbols, respectively. The ^{13}C pulses applied to C′ have the shape of the center lobe of a sin x/x function, whereas the C$^{\alpha}$ pulses are applied with a rectangular shape and field strength of $\Delta/\sqrt{15}$ (90°) and $\Delta/\sqrt{3}$ (180°), where Δ is the separation in Hz between the centers of the C$^{\alpha}$ and C′ chemical shift regions. Water-selective $\pi/2$ pulses serve to avoid saturating the water resonance. The transfer delays are adjusted to $\tau = 1/4J_{NH} \cong 2.7$ ms, $T = 1/2J_{NC} \cong 34$ ms, and $\Delta = 1/2J_{CC^{\alpha}} \cong 9.0$ ms. The short delays δ_1, δ_2, and δ_3 compensate for pulse or gradient durations. Pulsed field gradients, G_1, G_2, G_3, G_4, G_5, and G_6 are applied along the z-axis (PFG$_z$) with a gradient strength of approximately 20 G/cm and lengths ranging from 100 to 2000 μs, followed by a recovery delay of 100 μs. The relative durations of G_5 and G_6 are given by the gyromagnetic ratios of ^{1}H and ^{15}N as $G_5/G_6 = \gamma_H/\gamma_N$. For the *intra*-HNCA experiment quadrature detection in the ^{13}C (t_1) dimension is achieved by incrementing the phase φ_2 according to the STATES–TPPI method. For the ZQ/DQ *intra*-COHNCA experiment either φ_1 is incremented to obtain cross peaks at the ^{13}C frequencies $\omega_C \pm \lambda\omega_{C^{\alpha}}$ or φ_2 is incremented yielding cross peaks at $\omega_{C^{\alpha}} \pm \omega_C/\lambda$. In the ^{15}N ($t_2$) dimension sensitivity enhanced quadrature detection is used, where for each t_2 increment φ_3 (A) or φ_3 and φ_4 (B) are increased by 180° and the sign of G_5 is inverted.

carbonyls at time point (a). During the subsequent time period Δ the $^1J_{NC\alpha}$ and $^2J_{NC\alpha}$ couplings remain active in addition to the $^1J_{C'C\alpha}$ coupling, whereas the $^1J_{NC'}$ coupling has no influence on the $2N_yC'_y$ multiple-quantum coherence. At time point (b) the coherence $4N_yC'_xC^{\alpha}_z$ is selected by the 90° ^{15}N and ^{13}C′ pulses and the pulsed field gradient. If the delays T and Δ are adjusted to $1/(2^1J_{NC'})$ and $1/(2^1J_{C'C\alpha})$, respectively, the transfer amplitudes for the intraresidue (I_{intra}) and sequential (I_{seq}) coherence

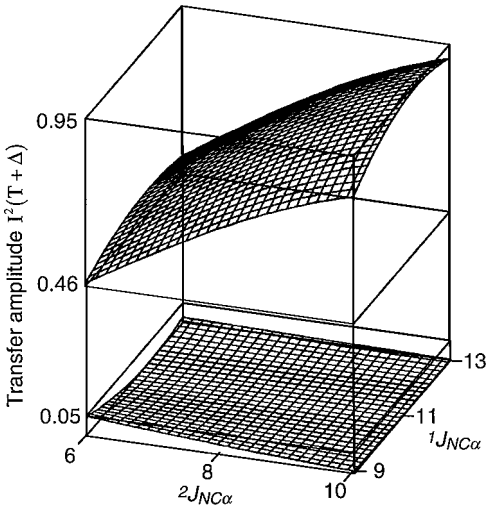

FIG. 2. Transfer amplitudes $I^2(T+\Delta)$ for the $^{15}N \rightarrow {}^{13}C$ transfer steps in the *intra*-(CO)HNCA experiments calculated using Eq. [1] for intraresidue (upper grid surface) and sequential (lower grid surface) correlations. Spin relaxation effects have been neglected for the calculation.

pathways are given by:

$$I_{\text{intra}}(T+\Delta) \propto \sin\left(\pi\, {}^1J_{NC\alpha}(T+\Delta)\right)\sin\left(\pi\, {}^2J_{NC\alpha}(T+\Delta)\right)$$
$$I_{\text{seq}}(T+\Delta) \propto \cos\left(\pi\, {}^1J_{NC\alpha}(T+\Delta)\right)\cos\left(\pi\, {}^2J_{NC\alpha}(T+\Delta)\right). \quad [1]$$

The $^1J_{NC\alpha}$ and $^2J_{NC\alpha}$ coupling constants can vary significantly from one residue to another (*13*) depending on local structure, hydrogen bonding, and other factors. The result of a numerical evaluation of the transfer amplitudes of intraresidue and sequential H–N–C^α cross peaks (Eq. [1]) as a function of the range of reported coupling constants $^1J_{NC\alpha}$ and $^2J_{NC\alpha}$ is shown in Fig. 2. The calculation takes into account that two identical $^{15}N \rightarrow {}^{13}C$ transfer steps are present in the pulse sequences of Fig. 1. For average values (*13*) measured in α helices ($^1J_{NC\alpha} = 9.6$ Hz, $^2J_{NC\alpha} = 6.4$ Hz) and β sheets ($^1J_{NC\alpha} = 10.9$ Hz, $^2J_{NC\alpha} = 8.3$ Hz) one obtains $I^2_{\text{intra}} = 0.54$ and $I^2_{\text{seq}} = 0.03$ for α helices, and $I^2_{\text{intra}} = 0.80$ and $I^2_{\text{seq}} = 0.002$ for β strand residues. These results indicate that the intensity of sequential cross peaks is expected to be generally well below 10% of the intensity of the intraresidue cross peak for the *intra*-HNCA and *intra*-COHNCA experiments. It is also interesting to compare these transfer amplitudes with a conventional HNCA experiment. For HNCA the $^{15}N \rightarrow {}^{13}C$ transfer amplitudes as a function of the transfer delay T are given by the equations:

$$I_{\text{intra}}(T) \propto \sin\left(\pi\, {}^1J_{NC\alpha}T\right)\cos\left(\pi\, {}^2J_{NC\alpha}T\right)$$
$$I_{\text{seq}}(T) \propto \cos\left(\pi\, {}^1J_{NC\alpha}T\right)\sin\left(\pi\, {}^2J_{NC\alpha}T\right). \quad [2]$$

For average coupling constants $^1J_{NC\alpha}$ and $^2J_{NC\alpha}$ found in regular secondary structural elements (see above) and a transfer delay of $T = 28$ ms one calculates (Eq. [2]) transfer amplitudes of $I^2_{\text{intra}} = 0.40$ and $I^2_{\text{seq}} = 0.13$ for α helices, and $I^2_{\text{intra}} = 0.37$ and $I^2_{\text{seq}} = 0.15$ for β strand residues. For the COHNCA experiment these values need to be corrected by a small factor $\sin^2(\pi\, {}^1J_{NC}T) = 0.94$ due to the additional J_{NC} coupling evolution. Compared to conventional techniques the new *intra*-(CO)HNCA experiments yield significantly higher transfer efficiency. The gain is most pronounced for β-strand residues characterized by large $^1J_{NC\alpha}$ and $^2J_{NC\alpha}$ coupling constants. An advantage in terms of sensitivity with respect to conventional pulse schemes is thus expected as long as the signal gain due to the increased $^{15}N \rightarrow {}^{13}C$ transfer amplitudes is higher than the signal loss due to spin relaxation during the longer transfer delays (43 ms for *intra*-HNCA instead of 28 ms for conventional HNCA).

The pulse sequence of Fig. 1A has been optimized for application to fully protonated or partially deuterated proteins. In the case of perdeuterated molecules and high magnetic field strengths (600-MHz ^{1}H frequency or higher) the ^{15}N TROSY (*14*) version of the experiments, shown in Fig. 1B, is preferable. In this sequence ^{15}N transverse relaxation is reduced by the TROSY effect which means less signal loss during the long $^{15}N \rightarrow {}^{13}C$ transfer delays. Because of additional $^{13}C'$ transverse relaxation during the delays Δ, which is dominated by the $^{13}C'$ chemical shift anisotropy mechanism, the experiments will perform best at magnetic field strengths of 600-MHz ^{1}H frequency or less. At higher magnetic fields the intrinsic sensitivity gain of the high field will be counterbalanced by the increased relaxation loss during the $^{15}N \rightarrow {}^{13}C$ transfer delays. The *intra*-HNCA experiment is thus complementary to the *sequential* HNCA experiment recently introduced by Meissner and Sørensen (*15*), which has been designed to correlate H(i), N(i), and $C^\alpha(i-1)$ nuclei and which becomes most attractive for application to large perdeuterated proteins at the highest available magnetic fields (800-MHz ^{1}H frequency or higher).

To demonstrate the performance of the new experiments 3D data sets of *intra*-HNCA and *intra*-COHNCA were recorded at 600-MHz ^{1}H frequency on a sample of uniformly ^{13}C, ^{15}N-labeled, and 77% ^{2}H labeled SiR-FP18, an 18-kDa (168 residues) functional fragment corresponding to the flavodoxin-like domain of the *Escherichia coli* sulfite reductase (*11*). For this sample the pulse sequences of Fig. 1A proved to be more sensitive than the corresponding ^{15}N TROSY version. Two-dimensional (^{1}H, ^{13}C) planes extracted from the recorded 3D spectra are shown in Fig. 3A for *intra*-HNCA and in Fig. 3C for *intra*-COHNCA. These spectra can be compared with spectra recorded using conventional HNCA and COHNCA pulse sequences shown in Figs. 3B and 3D, respectively. The correlation peaks of nine residues from different parts of the polypeptide chain are visible in these 2D spectral planes which allows a fair evaluation of the signal-to-noise and spectral resolution obtained with the new pulse sequences. The average signal-to-noise ratio of the intraresidue correlation peaks is very similar

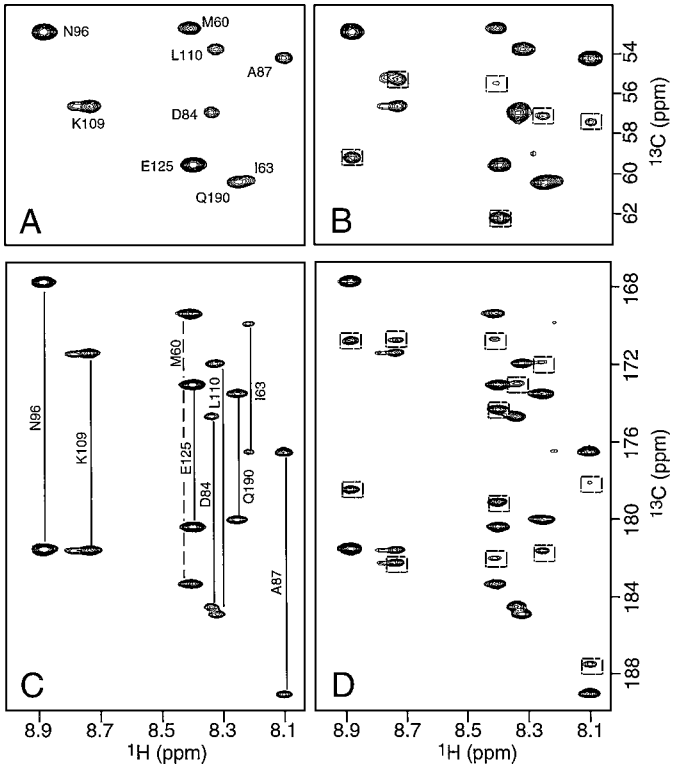

FIG. 3. 2D ^{1}H, ^{13}C planes from the 3D spectra of (A) *intra*-HNCA, (B) HNCA, (C) ZQ/DQ *intra*-COHNCA, and (C) ZQ/DQ COHNCA extracted at $\omega_N = 123.5$ ppm. The *intra*-HNCA and ZQ/DQ *intra*-COHNCA spectra were recorded using the pulse sequence of Fig. 1A. For the HNCA and ZQ/DQ COHNCA standard pulse sequences were used and the $^{15}N \rightarrow {}^{13}C$ transfer delays were set to 28 ms. ZQ/DQ frequency labeling of the C′ and C^{α} spins was achieved using quadrature detection of the C′ spins and setting the scaling factor to $\lambda = 0.5$. The C^{α} demodulation frequency was set to 67 ppm. All spectra were acquired on a 1.5-mM ^{13}C, ^{15}N, ^{2}H (77%) labeled sample of SiR-FP18 dissolved in 90% H_2O/10% D_2O (pH 7.0) at 600 MHz ^{1}H frequency and 30°C. For the HNCA and *intra*-HNCA experiments data sets of $100(^{13}C) \times 50(^{15}N) \times 512(^{1}H)$ complex points were recorded for spectral widths of 4500 (^{13}C), 1800 (^{15}N), and 9000 Hz (^{1}H) in an experimental time of 19 h. For the COHNCA and *intra*-COHNCA experiments the spectral width in the ^{13}C dimension was increased to 6000 Hz and 150 complex points were recorded in an experimental time of 38 h. The residue number annotates intraresidue correlation peaks in spectra (A) and (C), whereas dashed boxes highlight sequential correlation peaks detected in spectra (B) and (D). Note that not all observed cross peaks have their intensity maximum in the extracted 2D plane.

for the (CO)HNCA and *intra*-(CO)HNCA experiments. For most residues the relative intensity from *intra*-(CO)HNCA and conventional (CO)HNCA experiments varies within a range of about −50 to +50%, which is mainly explained by variations in the $^{1}J_{NC\alpha}$ and $^{2}J_{NC\alpha}$ coupling constants from one residue to another. A sensitivity gain of up to 100% is obtained by the *intra*-(CO)HNCA experiment for some flexible residues at the N and C terminus. For β-strand residues (e.g., N96 and K109) the cross peak intensity is generally increased in the *intra*-COHNCA spectrum, whereas for α-helical residues (e.g., D84, A87, and Q190) it is decreased. The new *intra*-(CO)HNCA experiments will compare most favorably for application to ^{13}C, ^{15}N labeled β-sheet rich proteins in the molecular weight range up to about 20 kDa or for perdeuterated higher molecular weight systems using the ^{15}N TROSY version of the experiments.

The principal characteristic of the *intra*-HNCA and *intra*-COHNCA experiments is that the sequential correlation peaks, clearly visible for most of the residues in Figs. 3B and 3D, are absent from the spectra of Figs. 3A and 3C. More quantitatively this means that the intensity of the sequential correlation peak is reduced to a few percent (or less) of the intensity of the corresponding intraresidue correlation peak. For the large majority of residues of SiR-FP18 the intensity is below the noise level as can be appreciated from 1D traces, shown in Fig. 4A, extracted from the 3D *intra*-HNCA spectrum along the ^{13}C dimension. The detection of only half the correlation peaks in the *intra*-(CO)HNCA spectra compared to conventional experiments significantly reduces the complexity of the spectra and thus facilitates the manual or computer-assisted spectral analysis.

In conclusion, the *intra*-HNCA (and *intra*-COHNCA) experiments allow unambiguous correlation of the amide $^{1}H(i)$ and $^{15}N(i)$ (and $^{13}C(i-1)$) frequencies with the $^{13}C^{\alpha}(i)$ carbon of the same residue. The experiments thus complement without redundancy the *sequential* information obtained from an HNCOCA-type experiment. Highest sensitivity is obtained when the experiments are performed at moderate magnetic field strength (500- or 600-MHz ^{1}H frequency). As such magnets are available in most biomolecular NMR laboratories the *intra*-HNCA and *intra*-COHNCA will add two attractive new experiments to the panoply of available triple-resonance experiments for backbone resonance assignment of proteins. Similar to the *sequential* correlation experiments of Meissner and Sørensen (*16*) the principle of *intraresidue* $N \rightarrow C^{\alpha}$ magnetization transfer can also be extended to HNCACB-type experiments designed for correlating the C^{β} carbons with the amide H and N of the same residue.

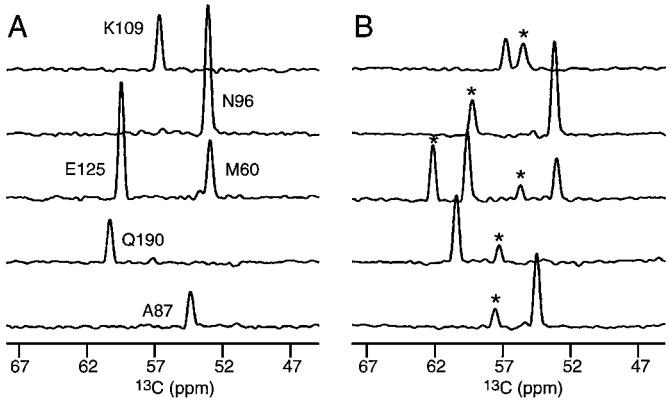

FIG. 4. 1D ^{13}C traces extracted from the (A) 3D *intra*-HNCA and (B) 3D HNCA spectrum of SiR-FP18 for some of the residues visible in the 2D planes of Fig. 3. The annotations in (A) indicate the corresponding residue, whereas the stars in (B) annotate additional sequential correlation peaks.

ACKNOWLEDGMENTS

The author thanks B. Bersch (IBS) and J. Covès (CEA, Grenoble) for the preparation of the labeled SiR-FP18 sample, and J.-P. Simorre for stimulating discussion. This work was supported by the Commissariat à l'Energie Atomique and the Centre National de la Recherche Scientifique. Continuing support from Accelrys Inc. (San Diego) is also acknowledged.

REFERENCES

1. M. Ikura, L. E. Kay, and A. Bax, A novel approach for sequential assignment of ^{1}H, ^{13}C, and ^{15}N spectra of larger proteins: Heteronuclear triple-resonance three-dimensional NMR spectroscopy. Application to calmoduline, *Biochemistry* **29,** 4659–4667 (1990).
2. A. Bax and S. Grzesiek, Methodological advances in protein NMR, *in* "NMR of Proteins" (G. M. Clore and A. M. Gronenborn, Eds.), pp. 33–52, Macmillan, London (1993).
3. K. H. Gardner and L. E. Kay, The use of ^{2}H, ^{13}C, ^{15}N multidimensional NMR to study the structure and dynamics of proteins, *Ann. Rev. Biophys. Biomol. Struct.* **27,** 357–406 (1998).
4. T. Szyperski, G. Wider, J. H. Bushweller, and K. Wüthrich, Reduced dimensionality in triple-resonance NMR experiments, *J. Am. Chem. Soc.* **115,** 9307–9308 (1993).
5. B. Brutscher, J.-P. Simorre, M. S. Caffrey, and D. Marion, Design of a complete set of two-dimensional triple-resonance experiments for assigning labeled proteins, *J. Magn. Reson. B* **105,** 77–82 (1994).
6. T. Szyperski, B. Banecki, D. Braun, and R. W. Glaser, Sequential resonance assignment of medium sized $^{15}N/^{13}C$-labeled proteins with projected 4D triple resonance NMR experiments, *J. Biomol. NMR* **11,** 387–405 (1998).
7. T. Szyperski, D. Braun, C. Fernandez, C. Bartels, and K. Wüthrich, A novel reduced-dimensionality triple-resonance experiment for efficient polypeptide backbone assignment, 3D COHNNCA, *J. Magn. Reson. B* **108,** 197–203 (1995).
8. B. Brutscher, F. Cordier, J.-P. Simorre, M. Caffrey, and D. Marion, High resolution 3D HNCOCA experiment applied to a 28 kDa paramagnetic protein, *J. Biomol. NMR* **5,** 202–206 (1995).
9. M. Caffrey, J.-P. Simorre, B. Brutscher, M. Cusanovich, and D. Marion, NMR assignment of Rhodobacter capsulatus ferricytochrome c′, a 28 kDa paramagnetic heme protein, *Biochemistry* **34,** 5904–5911 (1995).
10. B. Brutscher, R. Brüschweiler, and R.R. Ernst, Backbone dynamics and structural characterization of the partially folded A State of Ubiquitin by ^{1}H, ^{13}C, and ^{15}N nuclear magnetic resonance spectroscopy, *Biochemistry* **36,** 13043–13053 (1997).
11. N. Sibille, J. Covès, D. Marion, B. Brutscher, and B. Bersch, ^{1}H, ^{13}C, and ^{15}N assignment of the flavodoxin-like domain of the Escherichia coli sulfite reductase, *J. Biomol. NMR* **21,** 71–72 (2001).
12. D. Marion, N. Tarbouriech, R. W. Ruigrok, W. P. Burmeister, and L. Blanchard, Assignment of the ^{1}H, ^{15}N and ^{13}C resonances of the nucleocapsid-binding domain of the Sendai virus phosphoprotein, *J. Biomol. NMR* **21,** 75–76 (2001).
13. F. Delaglio, D. A. Torchia, and A. Bax, Measurement of ^{15}N-^{13}C J couplings in stapholococcal nuclease, *J. Biomol. NMR* **1,** 439–446 (1991).
14. K. Pervushin, R. Riek, G. Wider, and K. Wüthrich, Attenuated T_2 relaxation by mutual cancellation of dipole-dipole coupling and chemical shift anisotropy indicates an avenue to NMR structures of very large biological macromolecules in solution, *Proc. Natl. Acad. Sci. USA* **94,** 12366–12371 (1997).
15. A. Meissner and O. W. Sørensen, A sequential HNCA NMR Pulse Sequence for Protein Backbone Assignment, *J. Magn. Reson.* **150,** 100–104 (2001).
16. A. Meissner and O. W. Sørensen, Sequential HNCACB and CBCANH protein NMR pulse sequences, *J. Magn. Reson.* **151,** 328–331 (2001).